Journal of Medicinal Chemistry

Article

Fragment-based Discovery of New Highly Substituted 1H-Pyrrolo[2,3-b]- and 3H-Imidazolo[4,5-b]-Pyridines as Focal Adhesion Kinase Inhibitors

Timo Heinrich, Jeyaprakashnarayanan Seenisamy, Lourdusamy Emmanuvel, Santosh S. Kulkarni, Jörg Bomke, Felix Rohdich, Hartmut Greiner, Christina Esdar, Mireille Krier, Ulrich Grädler, and Djordje Musil

J. Med. Chem., **Just Accepted Manuscript** • Publication Date (Web): 08 Jan 2013

Journal of Medicinal Chemistry is published by the American Chemical Society. 1155 Sixteenth Street N.W., Washington, DC 20036

Fragment-based Discovery of New Highly Substituted 1H-Pyrrolo[2,3-b]- and 3H-Imidazolo[4,5-b]-Pyridines as Focal Adhesion Kinase Inhibitors

Timo Heinrich,[*,†] Jeyaprakashnarayanan Seenisamy,[‡] Lourdusamy Emmanuvel,[¥] Santosh S. Kulkarni,[‡] Jörg Bomke,[†] Felix Rohdich,[†] Hartmut Greiner,[†] Christina Esdar,[†] Mireille Krier,[†] Ulrich Grädler,[†] Djordje Musil[†]

[†] Merck Serono Research, Merck KGaA, 64271 Darmstadt, Germany

[‡] Syngene International Ltd., Biocon Park, Plot 2&3, Bommasandra-Jigani Link Road, Bangalore 560 099, India

[¥] Karunya University, Dept. of Chemistry, School of science and humanities, Coimbatore 641114, India

Abstract

Focal adhesion kinase (FAK) is considered as an attractive target for oncology and small molecule inhibitors are reported to be in clinical testing. In a surface plasmon resonance (SPR)-mediated fragment screening campaign we discovered bicyclic scaffolds like 1H-pyrazolo[3,4-d]pyrimidines binding to the hinge-region of FAK. By an accelerated knowledge-based fragment growing approach essential pharmacophores were added. The establishment of highly substituted unprecedented 1H-pyrrolo[2,3-b]pyridine derivatisations provided compounds with sub-micromolar cellular FAK inhibition potential. The combination of substituents on the bicyclic templates and the nature of the core structure itself have a significant impact on the compounds FAK selectivity. Structural analysis revealed that the appropriately substituted pyrrolo[2,3-b]pyridine induced a rare helical DFG-loop conformation. The discovered synthetic route to introduce three different substituents independently paves the way for versatile applications of the 7-azaindole core.

Introduction

FAK is a 125-kDa nonreceptor tyrosine kinase that modulates cell adhesion, migration, proliferation, and survival in response to extracellular signals.[1-4] The N-terminal FERM domain (4.1, ezrin, radixin, moesin) of FAK is composed of three sub-domains and regulates the kinase activity of FAK.[5-10] In the autoinhibited state, the FERM domain directly binds to the kinase C-lobe, impeding access to the ATP-binding site and protecting the activation loop from phosphorylation by Src. The inhibitory FERM–kinase interaction involves the F2 lobe of the FERM domain and a site of the C-lobe centered at Phe596.[6] The FERM domain has been shown to associate with integrins and growth factors, implying the important role of FAK in integrating diverse cellular

signalling pathways. In addition to being a key player in regulating normal cellular activities such as adhesion, migration and survival, FAK is also implicated in cancer cell invasion, metastasis and survival.[11-13] Accordingly, FAK inhibition is considered as an effective antineoplastic strategy by inducing apoptosis and sensitizing tumor cells to chemotherapy. A couple of FAK inhibitors with mono- and bi-cyclic core structures have been described, some even in clinical phase-1 testing.[14-21] Structurally very similar pyrimidines **I** (TAE-226),[22] **II** (PF-562271),[23] pyridine **III** (PND-1186)[24] and the pyrrolopyrimidine **IV**[25] are described as hinge-binders whereas Chloropyramine[26] and Y15[27] are anticipated to target the FAK-VEGFR-3 interface and the Y397 site, respectively.

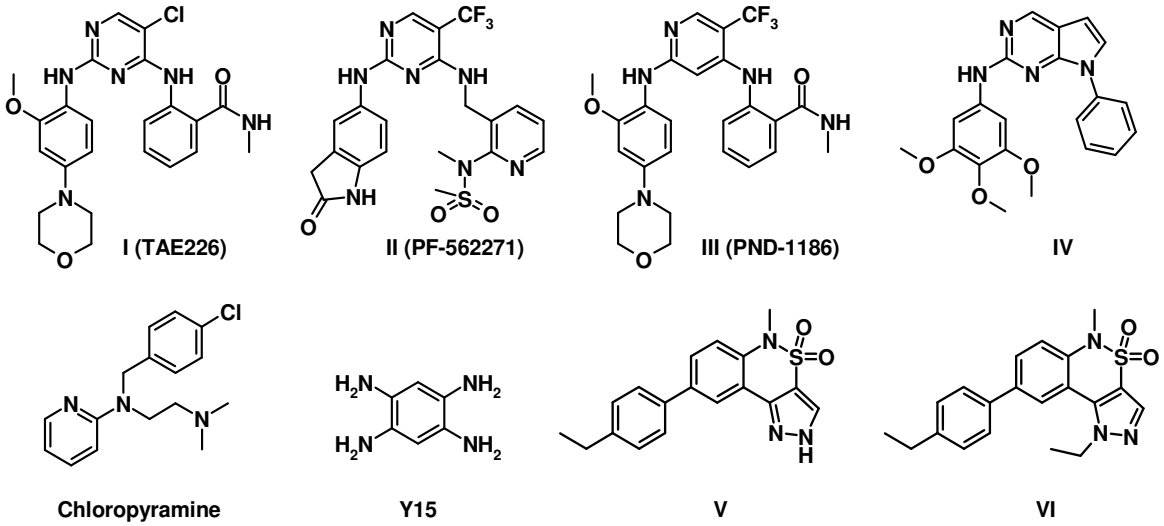

Figure 1. FAK inhibitors

Selective inhibition of protein kinases is a sometimes very difficult task in drug discovery research. Accordingly, drugs like sunitinib targeting the highly conserved ATP-binding pocket are multi-kinase inhibitors.[28] Allosteric kinase inhibition has been reported as an attractive option as enzyme blockade is achieved by addressing protein specific areas outside of the ATP-site.[29,30] Selective kinase inhibition of a ligand-template binding the backbone amides of the hinge region within the ATP-site might be achieved by shaping protein specific contacts or protein conformations. This was demonstrated for drugs such as imatinib, which bind to an inactive conformation of Abl kinase, adopting a particular conformation of the activation-loop.[31,32] This conformation is characterized by a rotation of the π-backbone torsion angle of the Asp in the DFG motif by approximately 180° ("DFG-out"). Imatinib's specificity has been attributed to its recognition of the DFG-out conformation of the Abl kinase activation loop.[33] For some FAK inhibitors like **II** or **III** bearing a pyrimidine or pyridine scaffold as hinge-binder, a remarkable FAK selectivity could be achieved and was explained by X-ray crystallography.[24,34,35] The crystal structure of FAK in complex with **II** revealed a helical conformation of the activation loop next to

Gly563, that is located ahead of the DFG-motif.[23] The high conformational flexibility of Gly563 and appropriately substituted ligands can force the activation loop of FAK into a helical conformation. Binding to this unusual kinase conformation is considered to be responsible for the inhibitor's selectivity as only 17 out of 90 tyrosine kinases have a Gly preceding the DFG motif.[36] In a very recent paper novel allosteric FAK inhibitors **V** and **VI** are described.[37] These sulphonamide based compounds inhibit unphosphorylated FAK more strongly than phosphorylated FAK by binding to the DFG-out conformation and inducing the unique HRD-loop conformation. This binding mode implicates steric occlusion of ATP-binding by activation loop residues Phe565 and Leu567, an inhibition mechanism also described for allosteric IGF-1R inhibitors.[30]

In this paper we introduce for the first time novel highly substituted bicyclic FAK inhibitors which induce a helical DFG-loop conformation of FAK.

Results

At the beginning of the project a set of commercially available fragments[38] was screened against the immobilized kinase domain of FAK.[39] The binding affinity was measured by SPR additionally enabling the determination of binding kinetics for most of the screened fragments.[40] Within a set of bicyclic screening hits (2-Fluoro-phenyl)-(1H-pyrazolo[3,4-d]pyrimidin-4-yl)-amine **1** was detected[41] with a K_D value of 43 µM.[42] The superimposed X-ray structures of FAK in complex with this fragment **1** (PDB ID: 4GU9) and with **II** (PDB ID: 3BZ3) are shown in figure 2.

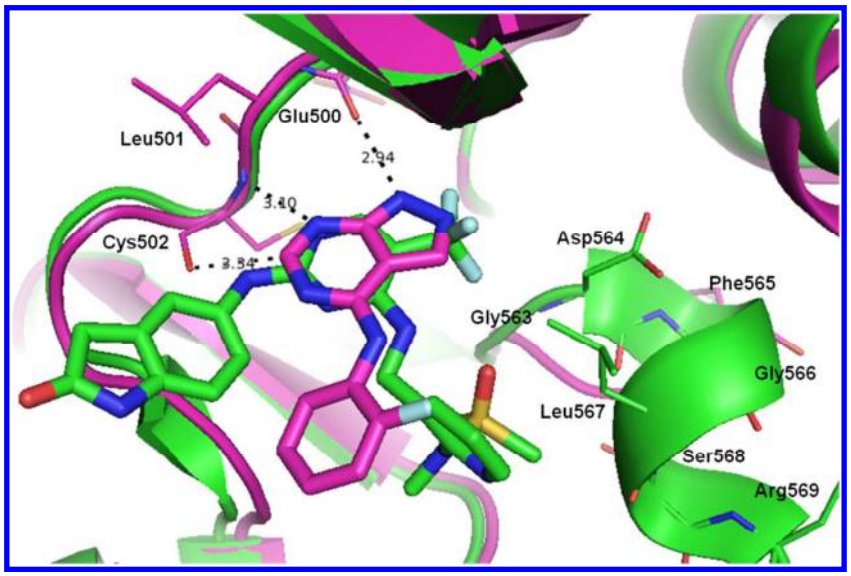

Figure 2. Superimposition of the FAK X-ray structures in complex with **II** (green, PDB ID: 3BZ3) and **1** (magenta, PDB ID: 4GU9, Monomer A) reveals hydrogen bond contacts (distances in Å) to backbone amides of Glu500 and Cys502 of the hinge-region. A non-classical H-bond is formed between the aromatic CH of **1** and

the carbonyl O-atom of Cyc502. In the FAK•II complex, the activation loop is partly (Asp564-Arg569) in a unique helical conformation.

The X-ray structure analysis reveals that both pyrimidine like nitrogens, N7 of **1** and N1of **II**, function as hydrogen-bond acceptors to the backbone-NH of Cys502 in the hinge region of the ATP-binding site. The exocyclic amino-group at C2 of the PF-compound is in hydrogen-bond distance of 2.83 Å to the backbone carbonyl-O of Cys502 whereas the hydrogen donor of fragment **1** is binding to the backbone carbonyl-O of Glu500 (2.94 Å). In addition the exocyclic amino-functions of fragment **1** and at C4 of **II** are equally oriented. Instead of the 1H-pyrazolo[3,4-d]pyrimidine scaffold of **1** the bicyclic system 1H-pyrrolo[2,3-b]pyridine was chosen as scaffold for the fragment growing work, as it offered various options for decoration (figure 3).

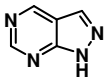

1H-pyrazolo[3,4-d]pyrimidine

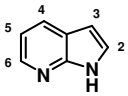

1H-pyrrolo[2,3-b]pyridine = 7-azaindole

Figure 3. Hinge-binding scaffold 1H-pyrazolo[3,4-d]pyrimidine of fragment **1** and 1H-pyrrolo[2,3-b]pyridine template selected for optimization as the lower nitrogen content of the later allows the introduction of more substituents.

A significant activity gain was achieved by introduction of a N-(3-Amino-methyl-pyridin-2-yl)-N-methyl-methanesulfonamide moiety in the 4-position of the 1H-pyrrolo[2,3-b]pyridine ring (**2**; K_D: 4.76 µM), which was previously described to interact with the rare helical DFG-loop conformation.[23] Based on these results scaffold modifications and residue extensions were realized to optimize the starting point **2**.

Two different strategies were followed to synthesize three-fold substituted pyrrolo[2,3-b]pyrimidines, with the objective to introduce residues as needed.[43] The first approach describes the de novo synthesis of the bicyclic scaffold structure (scheme 1) where as the second sequence was used for selective successive derivatisations of the 7-azaindole template (scheme 2). As depicted in scheme 1 commercially available 2-amino-pyridines **3** were applied in a Sonogashira coupling – base induced cyclisation sequence to prepare 2-substituted 7-azaindoles **4**, followed by selective halogenation of position 4 (**8**) and Buchwald amination (**11**). This Pd-catalysed last reaction worked best after pyrrolo-NH SEM protection (**10**).

Scheme 1: 7-Azaindoles by scaffold synthesis[a]

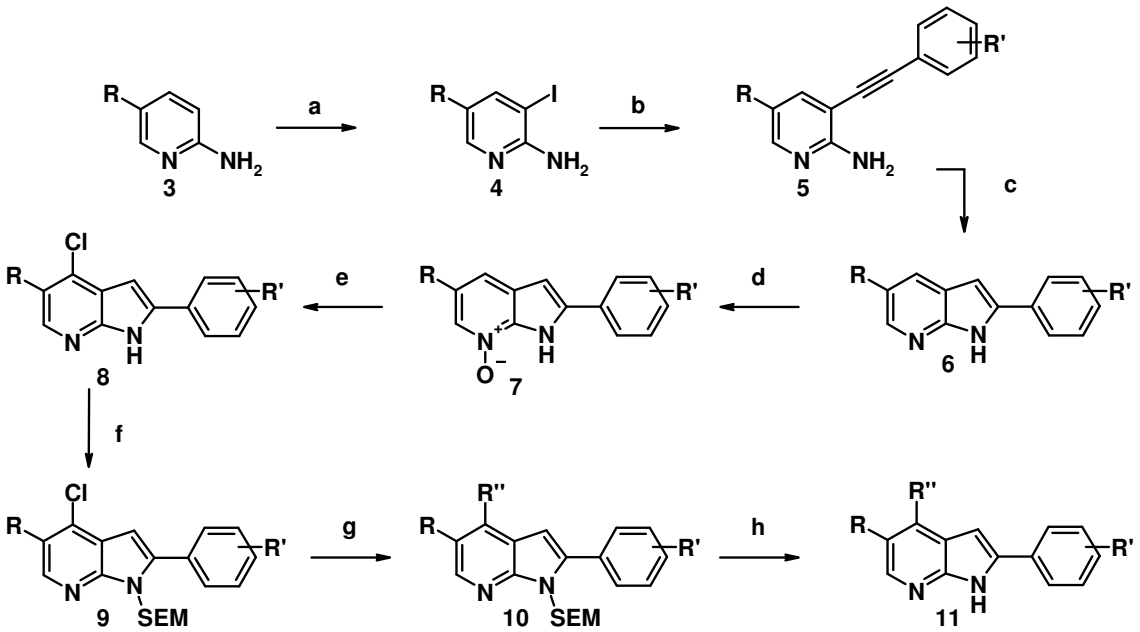

[a] Reaction conditions: R = CF_3, CN; (a) Ag_2SO_4, I_2; (b) R'-phenyl-ethin, $PdCl_2(PPh_3)_2$, CuI, DMF; (c) NaH, NMP, 60 °C; (d) m-CPBA; (e) $POCl_3$, MsCl, DMF; (f) SEM-Cl, DCM; (g) Cs_2CO_3, S-Phos, $Pd(OAc)_2$, R''-NH_2, dioxane, 150 °C; (h) 4N HCl, THF, reflux, 18 h.

This robust route suffers from the disadvantage that residues in position 2 of the final product have to be introduced at an early stage of the sequence and have to be compatible with challenging oxidative conditions. The alternative synthesis depicted in scheme 2 allows a more flexible approach to highly substituted 7-azaindoles without relying on harsh chemical reaction conditions.

Scheme 2: Synthesis of 7-azaindoles by selective and successive scaffold derivatisations[a]

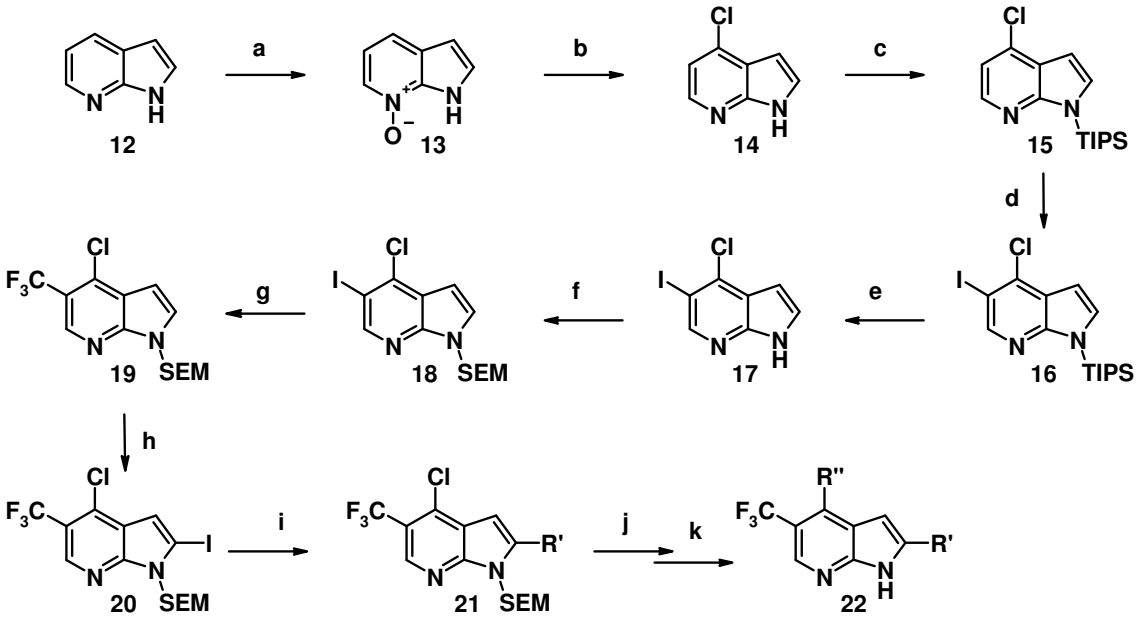

[a] Reaction conditions: (a) m-CPBA, 0 °C → RT, 77 %; (b) MsCl, DMF, 2 h, 50 °C, 72 %; (c) TIPS-Cl, NaH, THF, 1h, 0 °C, 65 %; (d) sec-BuLi, -78 °C, I_2, DMF, 60 %; (e) TBAF, THF, 1 h, 0 °C → RT, 80 %; (f) SEM-Cl, NaH, THF, 0 °C, 2h, 88 %; (g) 2,2-Difluoro-2-(fluorosulfonyl)acetic acid, CuI, DMF, 100 °C, 3 h, 72 %; (h) BuLi, -45 °C, I_2, THF, 64 %; (i) $Pd(OAc)_2$, S-Phos, Cs_2CO_3, R'-$B(OH)_2$, dioxane, H_2O, 60°C, 58 %; (j) $Pd(OAc)_2$, Xanthphos, Cs_2CO_3, R''-NH_2, dioxane, H_2O, 60 °C, 46 %; k. 4N HCl, THF, reflux, 65 %.

In a two-step sequence, commercially available 7-azaindole **12** is selectively chlorinated in positions 4 (**14**). Iodination in position 5 works best after TIPS protection of the pyrrole-nitrogen (**15**). Further transformations were only possible after protecting group exchange from TIPS (**16**) to SEM (**18**). Afterwards, the iodine substitution with CF_3 in position 5 (**19**) is possible, but also other residues like cyano can be introduced. Then the N-SEM protected 4-chloro-5-CF_3-7-azaindole **19** was lithiated in position 2 and quenched with iodine. The very versatile applicable building block **20** was used in selective Suzuki- and Buchwald coupling reactions and finally deprotected to allow access to novel highly decorated 7-azaindoles **22**. The introduction of a further heteroatom results in imidazo-pyridines **27**. The synthesis of these analogues was straightforward as outlined in scheme 3.[44]

Scheme 3: Synthesis of imidazopyridines 47-50[a]

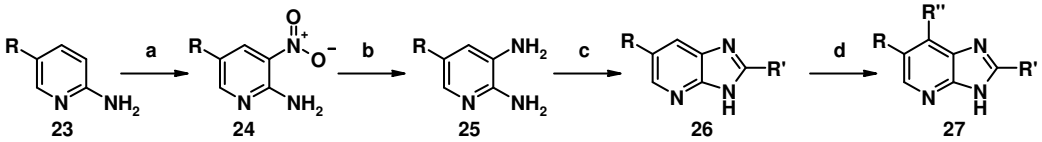

[a] Reaction conditions: (a) conc. H_2SO_4/HNO_3; (b) Fe, NH_4Cl; (c) R'-CHO, PTSA; (d)i: m-CPBA, $POCl_3$; ii: DIPEA, NMP, R''-NH_2.

Nitration of the amino-pyridine **23** derivative with appropriate substitution in position 3 followed by selective nitro reduction afforded the 2,3-diamino-pyridine building block **25** which could be reacted with aldehydes or acids under known conditions to the respective template **26**. Final Buchwald coupling gave the desired products **27**. SPR results of the imidazo- and pyrrolo-pyridines as well as results from biochemical and functional cellular assays are shown in table 1.

Table 1: Kinetic characterization as well as biochemical and cellular activities of the imidazo- and pyrrolo-pyridines.

	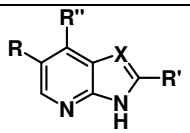				SPR Results		kinase assay[a]	HT-29[b]
No	**R**	**R'**	**R''**	**X**	K_D [nM]	k_d (off rate) [s^{-1}]	IC_{50} [nM]	IC_{50} [nM]
2[c]	H	H	N-(3-Amino-yl-methyl-pyridin-2-yl)-N-methyl-methanesulfonamide	C	4760	rco[d]	>10000	nd[e]
28[c]	CH_3				1700	0.56	8800	>10000
29	H	4F-phenyl			6380	0.80	4800	>10000
30	CH_3				554	0.071	910	>10000
31[c]	CN	H			147	0.40	2400	>10000
32[c]		Phenyl			44	0.022	195	1100± 700
33[c]		4F-phenyl			603	0.019	177	1300
34		Cy			242	0.12	>10000	nd[e]
35		4-nBu-Phe			430	0.028	>10000	nd[e]
36		(2-Me-Pyridin-4-yl)			24	mtl[f]	220	6500
37[c]	CF_3	4F-phenyl			24	0.011	37	2015 ± 750
38[c]			N-methyl-2-amino-yl-		nd[e]	nd[e]	51	552 ± 147

39[c]		pyridon-5-yl	benzamide		12	0.026	57	>10000
40[c]	CN	4F-phenyl			40	mtl[f]	37	365 ± 83
41[c]		4-morpholin-4-yl-phenyl			35	0.0026	45	83 ± 65
42[c]		6-morpholin-4-yl-pyridin-3-yl			9	0.0042	45	107 ± 12
43		4-morpholinyl-phenyl	3,5-difluoro-benzyl-amino		ddf[g]	ddf[g]	640	nd[e]
44	CF_3	4-morpholinyl-2-methoxy-phenyl	2-amino-yl-benzonitrile		1130	0.063	>10000	nd[e]
45			N-methyl-4-amino-yl-2,3-dihydro-isoindol-1-one		238	0.013	>10000	nd[e]
46		4F-phenyl	2,5-difluoro-benzyl-amino		ddf[g]	ddf[g]	>10000	nd[e]
47	Br		N methyl-2-amino-yl-benzamide		127	0.091	170	>10000
48[c]	CF_3		N-(3-Amino-yl-methyl-pyridin-2-yl)-N-methyl-methanesulfonamide	N	33	0.029	130	>10000
49		4-Br-Phe			189	0.034	700	>10000
50	Br	4F-phenyl			335	0.060	4500	>10000

[a]mean of three determinations, variations about ± 5%; [b]HT-29 cells possess a gene amplification of FAK and do therefore have high level of P-Y397-FAK; [c]selectivity data available, see table 2 and supporting information; [d]Rate constants outside instrument range; [e]not determined; [f]mass transfer limited data: kinetic constants cannot be unambiguously determined; [g]data don't fit to 1:1 model.

Discussion

Mono substituted azaindole **2** had shown micromolar affinity with transient binding kinetics (dissociation rate constant > 1 s^{-1}), but no biochemical inhibition below 10 µM could be measured for this compound. Attachment of a methyl group as second substituent in the 5-position of the 7-azaindole core (**28**) improved the affinity by

factor of 3 and an off-rate of 0.56 s^{-1} was measured.[45] By introduction of an aryl moiety like 4-fluoro phenyl in position 2 of **2**, the twofold substituted azaindole **29** was accessible. However, the binding affinities of **29** in comparison to **28** were somehow inconsistent as demonstrated by 3-fold higher K_D^{SPR} but a 2-fold lower biochemical IC_{50} value: affinity decreased but biochemical activity was improved slightly. Combination of the methyl group in position 5 and 4-fluoro-phenyl in position 2 resulted in the first example of a threefold substituted azaindole (**30**). Binding affinity measured by SPR and the biochemical IC_{50} of **30** were increased resulting in sub-micromolar values. As for **28** and **29**, no cellular activity could be found for **30**, indicating that an off-rate of 0.071 s^{-1} might be not sufficiently slow to achieve measurable target inhibition in HT-29 cells. Binding affinity could be more improved by the introduction of an electron withdrawing group in position 5 like cyano- (**31**) than with the electron donating methyl-substituent (**28**). While the K_D for **31** is 10-fold lower than for **28**, the off-rate was only slightly improved and biochemical activity was reduced by a factor of 4. The combination with an aryl moiety in position 2 like phenyl (**32**) or 4-fluoro-phenyl (**33**) improved activity further. K_D values for **32** and **33** differ nearly by one order of magnitude, whereas the off-rates are in the same range of about 0.02 s^{-1}. This is reflected by comparable cellular IC_{50}s of 1 µM for both compounds. Replacing the phenyl ring with cyclohexyl (**34**) or adding a further lipophilic moiety like n-butyl (**35**) abolished FAK inhibition in the enzymatic assay even though submicromolar K_D^{SPR} values of both compounds had suggested specific binding. The off-rate of **35** even points to cellular activity. This apparent inconsistency can be understood as **34** and **35** are virtually insoluble,[46] questioning biochemical and cellular data. Introduction of a heteroaryl moiety like pyridine (**36**) results in biochemical and cellular IC_{50} values comparable to the phenyl derivative **33**. Biophysical characterization of **36** was not possible as kinetic parameters could not be unambiguously determined. Switching from the linear cyano-function to the more bulky trifluoromethyl as residues in position 5 has a significant influence on the biochemical activity and resulted in the first two digit nanomolar FAK inhibitor from this series (**37**). The binding characterization revealed a K_D of 24 nM and a dissociation rate constant of 0.011 s^{-1}. This off-rate is only slightly decreased compared to **33** and no major improvement on the cellular activity could be expected. So far the aminomethyl-pyridine moiety in position 4 has been kept constant for the first optimisation rounds of R and R'. In another approach the amino-benzamide known from **I** was applied. Decoration with CF_3 in position 5 and 4-F-phenyl in position 2 did not alter biochemical activity but improved cellular FAK inhibition significantly exemplified by **38** as the first derivative with submicromolar cellular activity.[47] The 5-cyano analogue **40** is equally active than **38**, indicating a more pronounced influence on activity by substituents in position 4 (pointing to the FAK-DFG-area, vide infra) than in position 5 (gate-keeper interaction, vide infra). Binding to immobilized protein could only be interpreted partially for **40** as a K_D could be determined but no off-

rate was deducible from the data. Substitution of the aryl group in position 2 with morpholine finally resulted in further improvement of cellular activity as **41** and **42** have cellular IC_{50} in the 100 nM range. This is also reflected in the biophysical characterization, as these two derivatives have off-rates of 0.0026 s^{-1} and of 0.0042 s^{-1}, translating into residence times on the target of 6 and 4 minutes, respectively.[48] As acceptor functions like the sulphonamide or the benzamide in position 4 are beneficial for activity alternative acceptors were evaluated, too. The application of another literature known amino-aryl moiety, 4-amino-2,3-dihydro-isoindol-1-one,[49] in **45** which can be considered as a cyclic analogue of the amino-benzamide used for **38** – **42** gave very surprising results. Compound **45** did not show any activity in the biochemical assay, but the the K_D^{SPR} is still in the low three digit nanomolar range and the off-rate is only slightly higher than 0.01 s^{-1}. As **45** could be profiled in biophysical characterisation, low solubility of the derivative might be responsible for missing biochemical activity.[46] Other acceptor residues like the amino-benzonitrile (in **44**) or the fluoro-benzylamine (in **43**, **46**) did not improve FAK inhibition. Anyhow, surprisingly the 3,5-difluoro-benzylamine **43** is biochemically active in contrast to the cyclic amide **45**. The residues amino-benzamide and aminomethyl-pyridine which were used for the optimization of the pyrrolo[2,3-b]pyridine scaffold were also used for imidazo-pyridines **47** - **50**. As can be seen by comparing **48** with **37** the enzymatic activity is only three fold lower for the imidazo-derivative but no cellular activity could be found. This again is consistent with biophysical data as the off-rate is faster for **48**. For all imidazo-pyridines **47**- **50** the missing cellular activity can be understood when considering their off-rates ≥ 0.03 s^{-1}.

We assumed a favourable kinase selectivity profile for the 7-azaindole and imidazo-pyridine derivatives described in this paper, because the decorated rigid bicyclic scaffolds might have little flexibility to interact with different targets. For experimental confirmation of this hypothesis, an array of compounds (**2**, **28**, **31**-**33**, **37**-**42**, **48**) was chosen for selectivity profiling against 110 to 121 kinases. In table 2, we summarized the number of kinases inhibited with higher and 10% lower potency than FAK-IC_{50} by the respective compound.

Table 2: Kinase selectivity of tested the imidazo- and pyrrolo-pyridines.[a]

No	**2**	**28**	**31**	**32**	**33**	**37**	**38**	**39**	**40**	**41**	**42**	**48**
A[b]	10	32	27	20	23	1	1	4	1	8	5	10
B[c]	21	44	47	50	45	38	39	43	35	45	44	60

[a]detailed selectivity data and graphical visualisations are given in the supporting information, [b]the number of kinases inhibited by the compound with higher potency than FAK , [c]the number of kinases inhibited by the compound with 10% lower potency than FAK.

Pyrrolopyrimidine **2** which is decorated with the literature known sulphonamide bearing ligand is quite unselective and more active on non-FAK kinases. This can be understood as the hinge binder is small and might interact with altered orientations in different kinases. The derivatives **28**-**33** show increased FAK activity but no improved FAK selectivity. Extension of the core by aryl addition in position 2(**32** and **33**) was not sufficient to induce more selective FAK inhibition. Changing CN (**33**) to CF_3 (**37**) in position 5 of the 7-azaindole core improved on the inhibition of FAK activity as well as selectivity. Derivative **38** confirms the tendency within this compound class: 2-(4-F-phenyl)-5-CF_3-7-azaindole scaffold bears FAK selectivity tolerating different small residues in position 4. This is corroborated by **39** with slightly decreased selectivity by replacement of the 4-F-phenyl in position 2 with a pyridinone ring. The importance of 4-F-phenyl for FAK-selectivity is strengthened by **40** as in this derivative the CN functionality is reintroduced without loss of preference for FAK. Also **41** and **42** confirm the 4-F-phenyl trend. These compounds bear the CF_3 in position 5 and amino-phenyl-carboxamide in position 4, known from **38** to be beneficial for selectivity, but have 4-morpholino-phenyl in position 2 and are less selective than **38**. As pointed out, the effect of 4-F-phenyl on selectivity should not be overestimated as **33** is not a FAK specific inhibitor, indicating that selective target inhibition requires a well balanced presentation of all pharmacophores. The effect of the template structure for selectivity considerations is insinuated by **48**. This imidazo-pyridine core is substituted with the same moieties (CF_3, 4-F-phenyl, aryl-sulfonamide) as pyrrolo-pyridine compound **37** but is much less FAK selective.

The fragment growing initiative of **1** was accompanied by X-ray structure analyses and figure 3 depicts the X-ray structure of **32** binding to the hinge-region of FAK (PDB ID: 4GU6).[50-55]

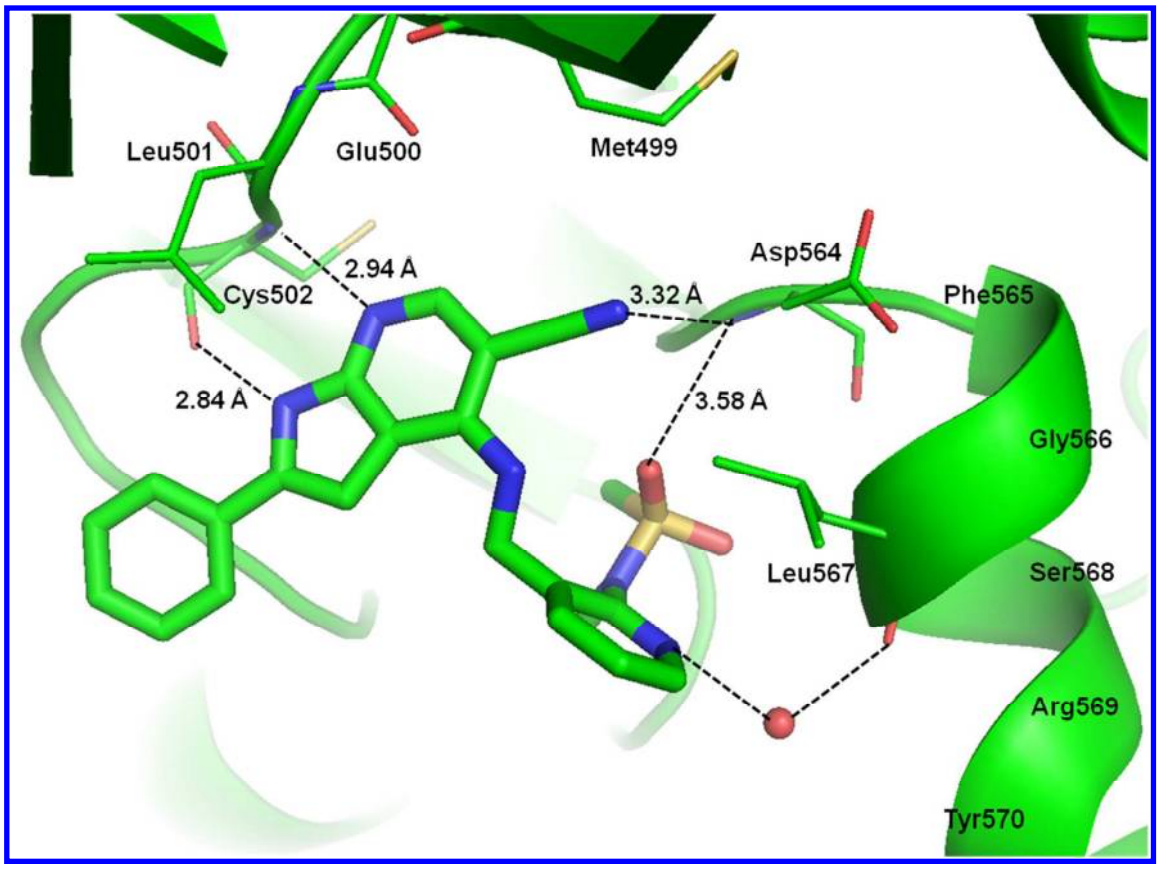

Figure 4: X-ray structure of FAK in complex with **32** indicates H-bond interactions to the hinge region (Cys502) and a rarely observed helical conformation of the activation-loop (Phe565-Tyr575; the helix is shown only partly until Tyr570 for clarity). Weaker H-bond contacts are formed between the cyano-nitrogen and the sulphonamide-oxygen of **32** and the Asp564 backbone-NH (distances in Å).

It is known that fragments can bind in different orientations to kinases and that binding mode can change in the growing process.[56,57] In a HCV dedicated approach for example, a benzoic acid fragment has even been described to flip by 180° after amide coupling.[58] In this work we also observed an inverted binding mode for the grown fragment. We were not surprised to see this difference in binding mode as the selected growing vector in **1** was pointing to the gatekeeper amino acid Met499, leaving not much space between protein and ligand. The anticipated hinge-interaction of N7 of **32** was confirmed by H-bond contacts to the backbone N-atom of Cys502. In contrast to the hydrogen donation of **1** to backbone carbonyl-O of Glu500, the 1H-NH of **32** bind to backbone carbonyl-O of Cys502. The CN-group of the 7-azaindole core is pointing towards gatekeeper residue Met499 and interacting with the backbone-NH of Asp564 from the DFG-motif. Also, one oxygen atom of the SO_2 group of **32** is in hydrogen-bond distance to the same backbone-NH of Asp564. Although both contacts are quite extended (3.32 & 3.58 Å) they might be responsible for the induction of the unusual activation loop

conformation, as described for **II**. Even though the phenyl residue in position 2 of the 7-azaindole is not interacting with lipophilic amino acid side chains the IC_{50} comparison of **32** with **31** proves that the aryl residue in **32** contributes to activity.

Conclusion

In an accelerated knowledge-based fragment-growing approach we decorated bicyclic hinge binding pyrrolo[3,4-d]pyridine in an unprecedented fashion. New chemical routes were discovered to enable selective and variable scaffold decorations even in late stages of the syntheses. Kinetic characterization and cellular testing of the selected compounds show that an off-rate of around 0.02 s^{-1} seems to be necessary for moderate cellular activity in HT-29 cells, while submicromolar cellular activity was only achieved with compounds having off-rates lower than 0.01 s^{-1}. Additionally, solubility and protein binding can disturb biochemical and cellular assays results even of compounds with confirmed FAK-binding by SPR. Here we have shown that the kinetic characterization of the compound-target interaction can deliver reliable data to ascertain the target activity of considered derivatives. In our fast knowledge-based fragment growing approach, starting from a hinge-binder it became obvious, that it was easier to improve kinase inhibition than kinase selectivity. We could show that the 4-F-phenyl substituent at the pyrrolopyridine is important for FAK selectivity. The described hit-series is a qualified starting point for a FAK dedicated hit-optimization program. Beyond the utilization of the described compounds in this targeted approach the unprecedented synthetic route can be used to get systematically highly substituted 7-azaindoles for alternative targets in medicinal chemistry.

Experimental Section.

Biology

FAK – Kinase Assay (autophosphorylation)

The Focal Adhesion Kinase (FAK) assay is performed as 384-well Flashplate assay. 2 nM FAK, 400 nM biotinylated substrate (His-TEV-hsFAK (31 – 686)(K454R) x Biotin) and 1 µM ATP (spiked with 0.25 µCi ^{33}P-ATP/well) are incubated in a total volume of 50 µl (60 mM Hepes, 10 mM $MgCl_2$, 1.2 mM Dithiothreitol, 0.02 % Brij35, 0.1 % BSA, pH 7.5) with or without test compound for 2 hours at 30 °C. The reaction is stopped with 25µl 200 mM EDTA. After 30 min at 30 °C the liquid is removed and each well washed thrice with 100 µl 0.9 % sodium chloride solution. Non-specific reaction is determined in presence of 1 µM PF-431396. Radioactivity is measured with a Topcount Microplate Scintillation Counter (Perkin Elmer). Results are calculated with Symyx Assay Explorer.

P-Y397-FAK Cellular Assay

HT29 cells which have gene amplification of FAK were plated at 30,000 cells/well in a 96-well microtiter plate and allowed to adhere overnight. Inhibitor compounds were added to each well in a 3-fold serial dilution (range from 30 µM to 0.03 µM) in triplicates for 45 min. After compound treatment, cells were lysed and cleared by centrifugation through a 96-well filter plate. FAK was captured from total lysates by incubation with a mouse-anti-FAK antibody (Merck Millipore, #05-537) coupled to Luminex microspheres overnight. The level of P-Y397-FAK was then detected by applying a rabbit-anti-P-Y397-FAK antibody (Sigma, #F7926) and an anti-rabbit-PE secondary antibody in a Luminex100 machine according to the manufacturer's instruction. Samples treated with DMSO vehicle were set as maximal phosphorylation and inhibitor treated samples were calculated as percent inhibition. Non-linear regression analysis (variable slope) was applied for determination of IC_{50} values (Accelry Assay Explorer).

Protein Crystallography

The construct FAK (411-686) was expressed and purified as described in the literature.[53] The protein was stored in a buffer containing 50 mM Tris/HCl, 250 mM NaCl, 1 mM EDTA, 1 mM DTT pH 7.6 and was concentrated to 6.5 mg/ml. FAK (410-689) P410G mutant was expressed and purified as described in the literature.[23] This protein construct was stored in 10 mM HEPES, 200 mM ammonium sulfate, 0.1 mM TCEP, pH 7.5 and was concentrated to 5.9 mg/ml. Crystals for the complex between **1** and the kinase domain (aa 410-686) of human recombinant FAK were prepared in the following way: FAK kinase domain was crystallized at 20 °C by hanging drop vapour diffusion against 0.1 M sodium citrate, pH 6.0, 18% PEG MME 2000. The protein was mixed 1:1 with the reservoir solution. For complex formation with the inhibitor, the crystals were transferred to a stabilizing solution (0.1 M sodium citrate, pH 6.0, 40 % PEG MME 2000) containing 5 mM **1**, 5 % DMSO and were soaked for 24 hours.

32 was co-crystallized with the kinase domain (aa 410-689) of the P410G mutant of human recombinant FAK at 20 °C by hanging drop vapour diffusion against 0.1 M Tris, pH 8.6 18 % PEG 3350, 200 µM **32**. The protein was mixed 1:1 with the reservoir solution.

X-ray diffraction data were collected on X06SA-PX beamline at Swiss Light Source (SLS) synchrotron radiation source using a Pilatus detector[50] and the images were indexed, integrated and scaled using XDS program package.[51] The data were collected using a cryo-cooled crystals at 90 K. The structure was solved by molecular replacement using the program MOLREP from the CCP4 program suite.[53] The structure 1mp8 from the Protein Data Bank (PDB)[59] was used as the search model. Subsequently, several cycles of refinement using the program Buster[54] and crystallographic model building using the graphic package COOT[55] were applied. The data collection and refinement statistics can be found in Table 3S.

Surface Plasmon Resonance (SPR)

The kinase domain of FAK was immobilized in the presence of an ATP-site specific inhibitor onto CM5 (series S) sensor chips using standard amine coupling. FAK inhibitor compounds (stored as 10 mM stock solutions in 100 % DMSO) were diluted in running buffer (10 mM HEPES, 150 mM NaCl, 5 mM $MgCl_2$, 1 mM DTT, 0.05 % Tween 20, 2 % DMSO pH 7,4) and analyzed with a Biacore 4000 or Biacore S51 (Biacore AB, GE Healthcare Life Sciences, Uppsala, Sweden) using a 2-fold dilution series. The highest compound concentration varied according to the expected dissociation constant, but all compounds were tested at 10 different concentrations. Interaction analysis cycles were run at 30 µL/min and consisted of a 180 s sample injection followed by 240 s of buffer flow (dissociation phase). All sensorgrams were evaluated by first subtracting the binding response recorded from the control surface (reference spot), followed by subtracting a buffer blank injection. To determine kinetic rate constants, data sets were fitted to a simple 1:1 interaction model including a term for mass transport using numerical integration and nonlinear curve fitting. Equilibrium analysis was performed by fitting the response at the end of the association phase to a single-site binding isotherm.

Chemistry. General Information: All reactions were carried out under nitrogen atmosphere or in sealed vials unless noted otherwise. Dry solvents and reagents were of commercial quality and were used as purchased. Reactions were magnetically stirred and monitored by thin-layer chromatography using Merck silica gel 60 F254 by fluorescence quenching under UV light or by LCMS detection, except if indicated otherwise. LCMS-analyses were run on Agilent 1100/1200 series) according to the following method: A-0.1 % TFA in H_2O, B-0.1 % TFA in ACN: Flow- 2.0 mL/min. on XBridge C8 (50 x 4.6mm, 3.5µm), +ve mode or Chromolith Performance RP18e. Retention times (Rt) are given in minutes. In addition, TLC plates were stained using phosphomolybdic acid or potassium permanganate stain. Chromatographic purification of products (flash chromatography) was performed on Isco Combiflash systems using Redisep columns and ethyl acetate/heptanes gradients. Concentration under reduced pressure was performed by rotary evaporation at 40 °C at the appropriate pressure unless otherwise stated. The purity of the compounds reported in the manuscript was established through HPLC-MS methodology. HPLC-analyses were run according to the LCMS method. ^{1}H-NMR (in DMSO-d6) and mass spectra are in agreement with the structures and were recorded on a Bruker AMX 400 MHz NMR spectrometer (TMS as an internal standard), and Vaccum Generators VG 70-70 or 70-250 at 70 eV, respectively. Elemental analyses (obtained with a Perkin-Elmer 240 BCHN analyser) for the final products were within 0.4 % of calculated values if not stated otherwise. All the compounds reported in the manuscript have a purity ≥ 95 % unless noted otherwise.

Syntheses as outlined in scheme 1 (R = CF_3; for others see supporting information)

*3-Iodo-5-(trifluoromethyl)pyridin-2-amine (**4**)*

5-(trifluoromethyl)pyridin-2-amine **3** (5.0 g, 30.8 mmol) was dissolved in 1,2-dichloroethane(50 mL) and silver trifluoroacetate (6.81 g, 30.8 mmol) was added. The suspension was refluxed for 7 h, after cooling to room temperature, iodine (7.8 g, 30.8 mmol) was added. The mixture was heated again for 12 h. After completion of the reaction, the reaction mixture was cooled to RT and the salt was removed by filtration. The filtrate was treated with water, extracted with DCM and the combined organic layer was dried over sodium sulphate and evaporated. The crude was purified by (60-120) silica gel chromatography to obtain **4** as brown solid in 56 % yield. ^{1}H-NMR: δ 8.26 (d, *J* = 1.12 Hz, 1H), 8.15 (d, *J* = 2.00 Hz, 1H), 6.88 (br s, 2H). LCMS: 289.0 (M+H), RT. 3.29 min, 91.93 % (Max), 93.21 % (254 nm).

*3-((4-Fluorophenyl)ethynyl)-5-(trifluoromethyl)pyridin-2-amine (**5**)*

To a degassed solution of **4** (2 g, 6.9 mmol) in dry DMF (35 mL), 4-fluoro phenyl acetylene (1.1 g, 8.7 mmol)**,** copper iodide (66 mg, 0.3 mmol), diisopropyl amine (2.9 mL) and dichlorobis(triphenylphospine)palladium (II) (0.243 g, 0.3 mmol) were added to a sealed tube and heated at 80 °C for 10 min. The reaction mixture was passed through celite and washed with 30 % methanol in dichloromethane (30 mL), the filtrate was concentrated and purified by column chromatography to get **5** as brown solid in 93 % yield. ^{1}HNMR: δ 8.28 (d, *J* = 1.44 Hz, 1H), 7.90 (d, *J* = 2.36 Hz, 1H), 7.73-7.77 (m, 2H), 7.26-7.31 (m, 2H), 7.17 (br s, 2H). LCMS: 281.0 (M+H), RT. 4.73 min, 99.17% (Max), 99.44 % (254 nm).

*2-(4-Fluorophenyl)-5-(trifluoromethyl)-1H-pyrrolo[2,3-b]pyridine (**6**)*

To a solution of potassium tert-butoxide (1.45 g, 12.8 mmol) in NMP under nitrogen, a solution of **5** (1.8 g, 6.4 mmol) in NMP (15 mL) was added drop wise at RT and the reaction mixture was heated at 120 °C for 12 h. The reaction was then quenched with water (50 mL) and extracted with ethyl acetate (50 mL) 3 times. The combined organic layer was washed with water, brine and was dried over anhydrous Na_2SO_4 to get **6** as yellow solid in 66 % yield. ^{1}H-NMR: δ 12.68 (br s, 1H), 8.55 (d, *J* = 0.68 Hz, 1H), 8.44 (d, *J* = 77.76 Hz, 1H), 8.01-8.04 (m, 2H), 7.33-7.38 (m, 2H), 7.06 (s, 1H). LCMS: 281.0 (M+H), RT. 5.03 min, 92.56 % (Max), 97.40 % (254 nm).

*2-(4-Fluorophenyl)-5-(trifluoromethyl)-1H-pyrrolo[2,3-b]pyridine 7-oxide (**7**)*

6 (1.2 g, 4.2 mmol) was suspended in acetone and cooled to 5 °C, *m*CPBA (0.83 g, 4.7 mmol) was added and the reaction mixture was stirred at RT for 12 h. The precipitate formed was then filtered and dried to get **7** as pale yellow solid in 39 % yield. ^{1}H-NMR: δ 13.45 (br s, 1H), 8.61 (d, *J* = 0.72 Hz, 1H), 8.10-8.13 (m, 2H), 8.05 (s, 1H), 7.31-7.35 (m, 2H), 7.16 (s, 1H). LCMS: 297.0 (M+H), RT. 3.95 min, 99.48 % (Max), 99.59 % (254 nm).

*4-Chloro-2-(4-fluorophenyl)-5-(trifluoromethyl)-1H-pyrrolo[2,3-b]pyridine (**8**)*

7 (0.5 g, 2.1 mmol) was taken in phosphorus oxychloride (10mL) and heated at 85 °C for 3 h. After the completion of reaction, excess phosphorus oxychloride was removed under high vacuum and the residue was diluted with cold water (5 mL) and basified with $NaHCO_3$ solution. The aqueous layer was extracted with ethyl acetate (25 mL), the combined organic layer was washed with water and followed by brine solution, and was dried over anhydrous Na_2SO_4, concentrated under reduced pressure to obtain **8** as a pale yellow solid which was taken to the next step without further purification (70 %). ^{1}H-NMR: δ 8.58 (s, 1H), 8.08-8.12 (m, 2H), 7.20-7.39 (m, 2H), 7.10 (s, 1H). LCMS: 315.0 (M+H), RT. 5.51 min, 97.70 % (Max), 97.12 % (254 nm).

*4-Chloro-2-(4-fluorophenyl)-5-(trifluoromethyl)-1-((2-(trimethylsilyl)ethoxy)methyl)-1H-pyrrolo[2,3-b]pyridine (**9**)*

A pre oven-dried two neck round bottom flask was charged with **8** (520 mg, 2 mmol) and dry THF (20 mL) at 0°C. Sodium hydride (60 % dispersion in mineral oil, 88 mg, 2.2 mmol) was added portion wise keeping the temperature below 5 °C and the resulting suspension was stirred at 0 °C for another 30 minutes followed by addition of SEM-Cl (365 mg, 2.2 mmol) drop wise. After the completion of the reaction, it was quenched with saturated ammonium chloride solution (5 mL) diluted with ethyl acetate (50 mL) washed with water, brine and dried over anhydrous Na_2SO_4. Concentration of the organic layer gave pale yellow oil which was purified by column chromatography to get **9** as colorless solid in 75 % yield. ^{1}H-NMR: δ 8.68 (s, 1H), 7.86-7.89 (m, 2H), 7.37-7.42 (m, 2H), 6.96 (s, 1H), 5.65 (s, 2H), 3.57 (t, J = 8.12 Hz, 2H), 0.81 (t, J = 7.96 Hz, 2H), (s, 9H). LCMS: 445.3 (M+H), RT. 7.342 min, 96.16 % (Max), 96.97 % (254 nm).

*7-azaindole N-Oxide (**13**)*

To a stirred solution of 7-azaindole **12** (50.0 g, 0.42 mol) in ethyl acetate (1.5 L) at 0 °C was added *m*CPBA (60 %) (144 g, 0.60 mol) portion wise over a period of 10 minutes and the reaction mixture was stirred for another 1 h. After the completion of the reaction the solid was filtered and dissolved in chloroform/methanol = 9:1 and neutralized with saturated Na_2CO_3 solution. The layers were separated and the organic layer was dried over anhydrous Na_2SO_4, concentrated under reduced pressure to get **13** as white solid in 60 % yield (34 g). ^{1}H-NMR: δ 12.47 (s, 1H), 8.10 (d, *J* = 6.12 Hz, 1H), 7.62 (dd, *J* = 1.80, 6.88 Hz, 1H), 7.44 (d, *J* = 3.28 Hz, 1H), 6.56 (d, *J* = 3.28 Hz, 1H).

*4-Chloro-1H-pyrrolo[2,3-b]pyridine (**14**)*

To a stirred solution of **13** (18.5 g, 0.14 mol) in DMF (150 mL) at 52°C was added methane sulfonyl chloride (32 mL, 0.41 mol) drop wise and the reaction mixture was heated to 72 °C for 2 h. After the completion of the reaction, the reaction mixture was poured over crushed ice and neutralized with 5M NaOH solution. The solid obtained was filtered and dried under vacuum to get **14** as orange color solid in 75 % yield (16 g). ^{1}H-NMR: δ

12.03 (s, H), 8.16 (d, *J* = 5.12 Hz, H), 7.58 (t, *J* = 3.00 Hz, H), 7.18 (d, *J* = 5.16 Hz, H), 6.49 (dd, *J* = 1.96, 3.44 Hz, H). LCMS: 153.0 (M+H), RT. 2.10 min, 93.4 % (Max), 93.6 % (254 nm).

*4-Chloro-1-triisopropylsilanyl-1H-pyrrolo[2,3-b]pyridine (**15**)*

To a stirred solution of **14** (16 g, 0.10 mol) in THF (300 mL) at 0 °C was added NaH (60 % in mineral oil, 5 g, 0.14 mol) portion wise and the mixture was stirred at the same temperature for 20 minutes, then triisopropyl silyl chloride (22.3 g, 0.16 mol) was added drop wise maintaining the temperature at 0 °C. After the reaction was complete, the reaction mixture was quenched with saturated NH_4Cl solution (10 mL) diluted with water and extracted with petroleum ether (3 × 200 mL). The crude compound was purified by column chromatography giving **15** as colorless liquid in 92 % yield (30 g). ^{1}H-NMR: δ 8.18 (d, *J* = 5.16 Hz, 1H), 7.59 (d, *J* = 3.80 Hz, 1H), 7.23 (d, *J* = 5.16 Hz, 1H), 6.67 (d, *J* = 3.52 Hz, 1H), 1.82-1.90 (m, 3H), 1.05 (d, *J* = 7.52 Hz, 18H). LCMS: 309.2 (M+H), RT. 7.56 min, 84.8 % (Max).

*4-Chloro-5-iodo-1-triisopropylsilanyl-1H-pyrrolo[2,3-b]pyridine (**16**)*

To a solution of **15** (11 g, 35.7 mmol) in THF (100 mL) at -78 °C was added sec-BuLi (53 mL, 78.5 mmol) drop wise over a period of 30 minutes and the reaction mixture was stirred for another 1h at the given temperature. A solution of iodine (18 g, 71.1 mmol) in THF (50 mL) was then added drop wise over a period of 30 minutes at the same temperature and the resulting suspension was stirred for 1 h and slowly brought to 0 °C. The reaction was quenched with saturated NH_4Cl solution, extracted with ethyl acetate, washed with water, brine, dried over Na_2SO_4 and concentrated under reduced pressure to get crude compound which was purified using petroleum ether by chromatography over silica gel to get **16** as a colorless liquid in 53 % yield (8.25 g). ^{1}H-NMR: δ 8.52 (s, 1H), 7.57 (d, *J* = 3.52 Hz, 1H), 6.67 (d, *J* = 3.48 Hz, 1H), 1.80-1.88 (m, 3H), 1.04 (d, *J* = 7.52 Hz, 18H). LCMS: 435.0 (M+H), RT. 7.98 min, 96.9 % (Max).

*4-chloro 5-iodo-1H-pyrrolo [2,3-b]pyridine (**17**)*

To a stirred solution of **16** (11 g, 25.3 mmol) in dry THF (200 mL) at 0 °C was added TBAF (1M solution in THF; 27 mL, 27 mmol) and allowed to stir for 30 minutes. After the completion of the reaction, the solvent was evaporated, diluted with ethyl acetate, washed with water, brine and dried over anhydrous Na_2SO_4. Concentration of the organic layer gave **17** as pale yellow solid in 99 % yield (7 g). ^{1}H-NMR: δ 12.15 (s, 1H), 8.50 (s, 1H), 7.58 (d, *J* = 3.40 Hz, 1H), 6.49 (d, *J* = 3.44 Hz, 1H), 5.09 (s, 1H). LCMS: 279.0 (M+H), RT. 3.97 min, 63.5 % (Max).

*4-chloro 5-iodo-1-(2-trimethylsilanyl-ethoxymethyl) -1H-pyrrolo [2,3-b]pyridine (**18**)*

A pre oven-dried two neck round bottom flask was charged with **17** (7 g, 25.2 mmol) and dry THF (75 mL) at 0 °C. Sodium hydride (60 % dispersion in mineral oil, 1.2 g, 32.5 mmol) was added portion wise keeping the

temperature below 5 °C and the resulting suspension was stirred at 0 °C for another 30 minutes followed by addition of SEM-Cl (5.03 g, 30.3 mmol) drop wise over a period of 15 minutes. After the completion of the reaction, it was quenched with saturated ammonium chloride solution (15 mL) diluted with ethyl acetate (100 mL) washed with water, brine and dried over anhydrous Na_2SO_4. Concentration of the organic layer gave **18** as pale yellow oil in 88 % yield 9 g). LCMS: 409.0 (M+H), RT. 6.51 min, 57.4 % (Max).

*4-chloro 5-trifluoromethyl-1-(2-trimethylsilanyl-ethoxymethyl) -1H-pyrrolo [2,3-b]pyridine (**19**)*

An oven dried two neck flask was charged with **18** (9 g, 22.1 mmol), cuprous iodide (4.2 g, 22.1 mmol), DMF (45 ml) and methyl 2,2-difluoro-2-(fluorosulfonyl)acetate (8.5 mL, 66.4 mmol). The resulting suspension was heated at 100°C for 2h. After the completion of the reaction, the copper residue was filtered off and the filtrate was extracted with ethyl acetate (100 mL) washed with water, brine and dried over anhydrous Na_2SO_4. Concentration of the organic layer gave the title compound as colorless solid which was purified by column chromatography using ether giving **19** in 59 % yield (4.6 g). ^{1}H-NMR: δ 8.64 (s, 1H), 7.98 (d, *J* = 3.6 Hz, 1H), 6.78 (d, *J* = 3.64 Hz, 1H), 5.67 (s, 2H), 3.49-3.53 (m, 2H), 0.78-0.82 (m, 2H), -0.14- -0.12 (m, 9H). LCMS: 351.0 (M+H), RT. 6.75 min, 43.3 % (Max).

*4-chloro-2-iodo- 5-trifluoromethyl-1-(2-trimethylsilanyl-ethoxymethyl) -1H-pyrrolo [2,3-b]pyridine (**20**)*

An oven dried two neck flask was charged with **19** (4.6 g, 13.1 mmol) and THF (50 mL) at -45 °C BuLi (1.6M stock solution in THF, 13.1 mmol) was added drop wise to the reaction mixture maintaining the temperature below -40 °C. The reaction mixture was stirred for another 30 minutes at the same temperature and I_2 (8.32 g, 32.7 mmol) solution in THF (25 mL) was then added drop wise. The reaction mixture was slowly brought to RT. After the completion of the reaction, it was quenched with saturated ammonium chloride solution, diluted with ethyl acetate (100 mL), washed with water, brine and dried over anhydrous Na_2SO_4. Concentration of the organic layer gave **20** as pale brown solid in 64 % yield (4 g) which was used without further purification. ^{1}H-NMR: δ 8.62 (s, 1H), 7.20 (s, 1H), 5.66 (s, 1H), 3.53 (t, *J* = 7.84 Hz, 2H), 0.81 (t, *J* = 7.9 Hz, 2H),-0.11 (s, 9H). LCMS: 477.0 (M+H), RT. 7.1 min, 74.6 % (Max).

Synthesis of *N-Methyl-2-[2-(6-morpholin-4-yl-pyridin-3-yl)-5-trifluoromethyl-1H-pyrrolo[2,3-b]pyridin-4-ylamino]-benzamide (**42**):*

4-Chloro-2-(6-morpholin-4-yl-pyridin-3-yl)-5-trifluoromethyl-1-(2-trimethylsilanyl-ethoxy methyl)-1H-pyrrolo[2,3-b]pyridine

To a 50 ml round bottom flask was added **20** (400 mg, 0.84 mmol), 6-(morpholin-4-yl) pyridine 3-boronic acid pinacol ester (290 mg, 1 mmol), Palladium acetate (19 mg, 0.084 mmol), S-Phos (34 mg, 0.084 mmol) and cesium carbonate (800 mg, 2.5 mmol). This mixture was suspended in dioxane (2.7 mL) and water (0.3 mL) and

heated at 60 °C for 12 h. The reaction was cooled to room temperature diluted with water (10 mL) and ethyl acetate (20 mL) and extracted with ethyl acetate (20 mL). The combined organic layer was washed with water (100 mL) and brine solution, then dried over anhydrous Na_2SO_4 and evaporated. The residue was purified by column chromatography to get title compound in 58 % yield (250 mg) as pale brown oil. ^{1}H-NMR: δ 8.65 (s, 1H), 8.57 (d, *J* = 2.3 Hz, 1H), 8.00-8.03 (m, 1H), 7.00 (d, J = 7.8 Hz, 1H), 6.94 (s, 1H), 5.66 (s, 2H), 3.70-3.72 (m, 4H), 3.56-3.63 (m, 6H), 0.82-0.86 (m, 2H),-0.11 (s, 9H).

N-Methyl-2-[2-(6-morpholin-4-yl-pyridin-3-yl)-5-trifluoromethyl-1-(2-trimethylsilanyl-ethoxymethyl)-1H-pyrrolo[2,3-b]pyridin-4-ylamino]-benzamide

To a 50 mL round bottom flask with stir bar was added 4-chloro-2-(6-morpholin-4-yl-pyridin-3-yl)-5-trifluoromethyl-1-(2-trimethylsilanyl-ethoxymethyl)-1H-pyrrolo[2,3-b]pyridine (80 mg, 0.156 mmol), 2-amino-N-methyl-benzamide (23 mg, 0.156 mmol), cesium carbonate (148 mg, 0.468) and dioxane (2 mL). The suspension was degassed using argon. XanthPhos (18 mg, 0.031 mmol) and Palladium acetate (7 mg, 0.031 mmol) were added and the reaction mixture was heated at 100 °C for 12 h. The reaction was then cooled to room temperature diluted with ethyl acetate (30 mL) and filtered through celite pad. Water (20 mL) was added, filtrated and extracted with ethyl acetate (60 mL). The combined organic layer was washed with water (50 mL) and brine solution, then dried over anhydrous Na_2SO_4 and evaporated. The residue was purified by column chromatography to get the title compound as viscous yellow liquid in 46 % yield (45 mg). LCMS: 626.8 (M+H), RT. 5.24 min, 74.7 %

*N-Methyl-2-[2-(6-morpholin-4-yl-pyridin-3-yl)-5-trifluoromethyl-1H-pyrrolo[2,3-b]pyridin-4-ylamino]-benzamide (**42**)*

To a solution of N-Methyl-2-[2-(6-morpholin-4-yl-pyridin-3-yl)-5-trifluoromethyl-1-(2-trimethylsilanyl-ethoxymethyl)-1H-pyrrolo[2,3-b]pyridin-4-ylamino]-benzamide (30 mg, 0.047 mmol) in THF (2 mL) was added HCl solution in dioxane (4N, 0.25 mL) and heated at reflux for 5 h. After completion of the reaction, the solvent was evaporated; the residue was dissolved in ethyl acetate (15 mL) and neutralized with saturated Na_2CO_3 solution. The organic layer was separated, washed with water, brine and dried over anhydrous Na_2SO_4 and evaporated. The residue was purified by column chromatography to get **42** as off white solid in 65 % yield (12 mg). ^{1}H-NMR: δ 12.40 (d, *J* = 2.00 Hz, 1H), 10.57 (s, 1H), 8.69 (d, *J* = 3.60 Hz, 1H), 8.51 (d, *J* = 3.0 Hz, 1H), 8.37 (s, 1H), 7.83-7.85 (m, 1H), 7.72-7.74 (m, 1H), 7.33-7.37 (m, 1H), 7.03 (t, *J* = 6.80 Hz, 1H), 6.97 (d, *J* = 8.28 Hz, 1H), 6.88 (d, *J* = 8.88 Hz, 1H), 5.99 (d, *J* = 2.20 Hz, 1H), 3.67-3.69 (m, 4H), 3.47-3.50 (m, 4H), 2.79 (d, *J* = 4.52 Hz, 3H). LCMS: 497.2 (M+H), RT. 2.85 min, 93.2 % (Max), 92.4 % (254 nm). HPLC: RT 2.79 min, 94.2 % (Max), 95.1 % (254 nm).

ASSOCIATED CONTENT

Supporting Information

Synthesis and characterization of intermediates from schemes 1, 2 and 3 & from table 1. Crystallographic data, refinement parameters, electron density maps for both respective monomers of **1** and **32**; selectivity data for **2**, **28**, **31**-**33**, **37**-**42**, **48** are given also visualization of **II** binding to FAK and kinetic data for **II**. This material is available free of charge via the Internet at http://pubs.acs.org.

Accession codes

X-ray structures of **1** (4GU9) and **32** (4GU6) bound to FAK have been deposited in the PDB (www.pdb.org).[59]

AUTHOR INFORMATION

Corresponding author

Email: timo.heinrich@merckgroup.com; phone: +49 6151 79 85 89; fax: +49 6151 72 31 29; URL: http://www.merckgroup.com

Notes:

The authors declare no competing financial interest

ACKNOWLEDGEMENTS

We acknowledge Michael Krug how helped in the visualization of the selectivity data

ABBREVIATIONS USED

BuLi, n-Butyllithium; DCM, Dichloromethane; DIPEA, Diisopropylethylamine; DMA, Dimethylacetamide; DMF, Dimethylformamide; DMSO, dimethylsulfoxide; DTT, dithiothreitol; EtOAc, Ethyl acetate; EtOH, Ethanol; FAK, Focal adhesion kinase; HEPES, 4-(2-hydroxyethyl)-1-piperazineethanesulfonic acid; LCMS: High-pressure liquid chromatography with subsequent mass detection; *m*CPBA, meta-Chloroperoxybenzoic acid; MeOH, Methanol; MsCl, Methanesulfonyl chloride; NMP, N-Nethylpyrrolidinone; PDB, protein data base; PTSA, para-Toluenesulfonic acid; RT, Roomtemperature; Rt, Retention time; SEM, Trimethylsilylmethoxymethyl; S-Phos, 2-Dicyclohexylphosphino-2',6'-dimethoxybiphenyl; SPR, Surface plasmon resonance; TFA, Trifluoroacetic acid; THF, Tetrahydrofurane; TIPS, Triisopropylsilyl; TLC, Thin layer chromatography; Xanthphos, 4,5-Bis(diphenylphosphino)-9,9-dimethylxanthene

REFERENCES

(1) Hall, J.E.; Fu, W.; Schaller, M.D. Focal Adhesion Kinase: Exploring FAK Structure to Gain Insight into Function. *Int. Rev. Cell Molecular Biol*. **2011**, *288*, 185–225.

(2) Peng, X.; Guan, J-L. Focal adhesion kinase: from in vitro studies to functional analyses in vivo. *Curr. Protein Pept. Sci*. **2011**, *12*, 52-67.

(3) Hochwald, S.N.; Golubovskaya, G.V. FAK as a target for cancer therapy. *Gene Ther. Mol. Biol*. **2009**, *13*, 26-35.

(4) Schlaepfer, D.D.; Mitra, S.K. Multiple connections link FAK to cell motility and invasion. *Curr Opin. Genet. Dev*. **2004**, *14*, 92-101.

(5) Corsi, J.M.; Rouer, E.; Girault, J.A.; Enslen, H. Organization and posttranscriptional processing of focal adhesion kinase gene. *BMC Genomics*. **2006**, *7*, 1-21.

(6) Frame, M.C.; Patel, H.; Serrels, B.; Lietha, D.; Eck, M.J. The FERM domain: organizing the structure and function of FAK. *Nat. Rev. Mol. Cell Biol.* **2010,** *11*, 802-814.

(7) Schaller, M.D. Biochemical signals and biological responses elicited by the focal adhesion kinase. *Biochim. Biophys. Acta* **2001**, *1540*, 1-21.

(8) Lim, S.-T.; Mikolon, D.; Stupack, D. G.; Schlaepfer, D. D. FERM control of FAK function. *Cell Cycle* **2008**, *7*, 2306-2314.

(9) Cooper, L. A.; Shen, T.-L., Guan, J.-L. Regulation of Focal Adhesion Kinase by Its Amino-Terminal Domain through an Autoinhibitory Interaction. *Mol. Cell. Biol.* **2003**, *23*, 8030-8041.

(10) Lietha, D.; Cai, X.; Ceccarelli, D.F.J.; Li, Y.; Schaller, M.D.; Eck, M.J. Structural Basis for the Autoinhibition of Focal Adhesion Kinase. *Cell* **2007**, *129*, 1177-1187.

(11) Cance, W.G.; Harris, J.E.; Iacocca, M.V.; Roche, E.; Yang, X.; Chang, J.; Simkins, S.; Xu, L. Immunohistochemical analyses of focal adhesion kinase expression in benign and malignant human breast and colon tissues: correlation with preinvasive and invasive phenotypes. *Clin. Cancer Res.* **2000**, *6*, 2417-2423.

(12) McLean, G.W.; Carragher, N.O.; Avizienyte, E.; Evans, J.; Brunton, V.G.; Frame, M.C. The role of focal-adhesion kinase in cancer - a new therapeutic opportunity. *Nat. Rev. Cancer* **2005**, *5*, 505-515.

(13) Golubovskaya, V. M.; Kweh, F. A.; Cance, W. G. Focal adhesion kinase and cancer. *Histol. Histopathol*. **2009**, *24*, 503-510.

(14) Infante, J. R.; Camidge, D. R.; Mileshkin, L. R.; Chen, E. X.; Hicks, R. J.; Rischin, D.; Fingert, H.; Pierce, K. J.; Xu, H.; Roberts, W. G.; Shreeve, S. M.; Burris, H. A.; Siu, L. L. Safety, Pharmacokinetic, and Pharmacodynamic Phase I Dose-Escalation Trial of PF-00562271, an Inhibitor of Focal Adhesion Kinase, in Advanced Solid Tumors *J. Clin. Onc.* **2012,** *30*, 1527-1533.

(15) Ucar, D. A.; Hochwald, S. N. FAK and interacting proteins as therapeutic targets in pancreatic cancer. *Anti-Cancer Agents Med. Chem.* **2010***, 10,* 742-746.

(16) Hochwald, S.N.; Nyberg, C.; Zheng, M.; Zheng, D.; Wood, C.; Massoll, N.A.; Magis, A.; Ostrov, D.; Cance, W.G.; Golubovskaya, V.M. A novel small molecule inhibitor of FAK decreases growth of human pancreatic cancer. *Cell Cycle* **2009**, *8*, 2435-2443.

(17) Liu, W.; Bloom, D.A.; Cance, W.G.; Kurenova, E.V.; Golubovskaya, V.M.; Hochwald, S.N. FAK and IGF-IR interact to provide survival signals in human pancreatic adenocarcinoma cells. *Carcinogenesis* **2008**, *29*, 1096-1107.

(18) Zheng, D.; Golubovskaya, V.M.; Kurenova, E.; Wood, C.; Massoll, N.A.; Ostrov, D.; Cance, W.G.; Hochwald, S.N. A novel strategy to inhibit FAK and IGF-1R decreases growth of pancreatic cancer xenografts. *Mol. Carcinog.*, **2010**, *49*, 200-209.

(19) de Courcy, B.; Piquemal, J.-P.; Garbay, C. ; Gresh, N. Polarizable Water Molecules in Ligand-Macromolecule Recognition. Impact on the Relative Affinities of Competing Pyrrolopyrimidine Inhibitors for FAK Kinase. *J. Am. Chem. Soc*. **2010**, *132*, 3312–3320.

(20) Kyu-Ho Han, E.; McGonigal, T. Role of Focal Adhesion Kinase in Human Cancer: A Potential Target for Drug Discovery. *Anti-Cancer Agents in Med. Chem.* **2007***, 7,* 681-684.

(21) Slack-Davis, J.-K.; Martin, K. H.; Tilghman, R. W.; Iwanicki, M.; Ung, E. J.; Autry, C.; Luzzio, M. J.; Cooper, B.; Kath, J.C.; Roberts, W. G.; Parsons, J. T. Cellular Characterization of a Novel Focal Adhesion Kinase Inhibitor. *J. Biol. Chem.* **2007**, *282*, 14845–14852.

(22) Halder J.; Lin Y. G.; Merritt W. M.; Spannuth W. A.; Nick A. M. Therapeutic efficacy of a novel focal adhesion kinase inhibitor TAE226 in ovarian carcinoma. *Cancer Res.* **2007**, *67*, 10976–10983.

(23) Roberts, W. G.; Ung, E.; Whalen, P.; Cooper, B.; Hulford, C.; Autry, C.; Richter, D.; Emerson, E.; Lin, J.; Kath, J.; Coleman, K.; Yao, L.; Martinez-Alsina, L.; Lorenzen, M.; Berliner, M.; Luzzio, M.; Patel, N.; Schmitt, E.; LaGreca, S.; Jani, J.; Wessel, M.; Marr, E.; Griffor, M.; Vajdos, F. Antitumor Activity and Pharmacology of a Selective Focal Adhesion Kinase Inhibitor, PF-562,271. *Cancer Res.* **2008**; *68*, 1935–1944.

(24) Walsh, C.; Tanjoni, I.; Uryu, S.; Tomar, A.; Nam, J.-O.; Luo, H.; Phillips, A.; Patel, N.; Kwok, C.; McMahon, G.; Stupack, D. G.; Schlaepfer, D. D. Oral delivery of PND-1186 FAK inhibitor decreases tumor growth and spontaneous breast to lung metastasis in pre-clinical models. *Cancer Biol. Ther.* **2010**, *9*, 1-13.

(25) Choi, H.-S-; Wang, Z.; Richmond, W.; He, X.; Yang, K.; Jiang, T.; Sim, T.; Karanewsky, D.; Gu, X.-j.; Zhou, V.; Liu, Y.; Ohmori, O.; Caldwell, J.; Graya, N.; He, Y. Design and synthesis of 7H-pyrrolo[2,3-d]pyrimidines as focal adhesion kinase inhibitors. *Bioorg. Med. Chem. Lett.* **2006**, 16, 2173–2176.

(26) Kurenova, E. V.; Hunt, D. L.; He, D.; Magis, A. T.; Ostrov, D. A.; Cance, W. G. Small Molecule Chloropyramine Hydrochloride (C4) Targets the Binding Site of Focal Adhesion Kinase and Vascular

Endothelial Growth Factor Receptor 3 and Suppresses Breast Cancer Growth in Vivo. *J. Med. Chem.* **2009**, *52*, 4716–4724.

(27) Golubovskaya, V. M.; Nyberg, C.; Zheng, M.; Kweh, F.; Magis, A.; Ostrov, D.; Cance, W. G. A Small Molecule Inhibitor, 1,2,4,5-Benzenetetraamine Tetrahydrochloride, Targeting the Y397 Site of Focal Adhesion Kinase Decreases Tumor Growth. *J. Med. Chem.* **2008**, *51,* 7405–7416.

(28) Roskoski Jr, R. Sunitinib: A VEGF and PDGF receptor protein kinase and angiogenesis inhibitor. *Biochem. Biophys. Res. Comm.* **2007**, *356*, 323–328.

(29) Barrett, S.D.; Bridges, A. J.; Dudley, D. T.; Saltiel, A. R.; Fergus, J. H.; Flamme, C. M.; Delaney, A. M.; Kaufman, M.; LePage, S.; Leopold, W. R.; Przybranowski, S. A.; Sebolt-Leopold, J.; Van Becelaere, K.; Doherty, A. M.; Kennedy, R. M.; Marston, D.; Howard, W. A, Jr; Smith, Y.; Warmus. J. S.; Tecle, H. The discovery of the benzhydroxamate MEK inhibitors CI-1040 and PD 0325901. *Bioorg. Med. Chem. Lett.* **2008**, *18*, 6501–6504.

(30) Heinrich, T.; Grädler, U.; Böttcher, H.; Blaukat, A.; Shutes, A. Allosteric IGF-1R Inhibitors. *ACS Med. Chem. Lett.* **2010**, *1*, 199–203.

(31) Nagar, B.; Bornmann, W. G.; Pellicena, P.; Schindler, T.; Veach, D. R. Crystal structures of the kinase domain of c-Abl in complex with the small molecule inhibitors PD173955 and imatinib (STI-571). *Cancer Res.* **2002**, *62*, 4236–4243.

(32) Nagar, B.; Hantschel, O.; Young, M. A.; Scheffzek, K.; Veach, D. Structural basis for the autoinhibition of c-Abl tyrosine kinase. *Cell* **2003**, *112*, 859–871.

(33) Seeliger, M. A.; Nagar, B.; Frank, F.; Cao, X.; Henderson, M. N. c-Src binds to the cancer drug imatinib with an inactive Abl/c-Kit conformation and a distributed thermodynamic penalty. *Structure* **2007**, *15*, 299–311.

(34) Lietha, D.; Eck, M.J. Crystal Structures of the FAK Kinase in Complex with TAE226 and Related Bis-Anilino Pyrimidine Inhibitors Reveal a Helical DFG Conformation. *PLoS ONE* **2008***, 3*, e3800, 1-7.

(35) Heinrich, T.; Brugger, N.; Rohdich, F.; Esdar, C.; Greiner, H.; Krier, M.; Seenisamy, J.; Jayadevan, J.; Sundararaman, V.-r. New Highly Selective FAK Inhibitors. P421, ISMC Berlin **2012**.

(36) Manning, G.; Whyte, D. B.; Martinez, R.; Hunter, T.; Sudarsanam, S. The protein kinase complement of the human genome. *Science* **2002**, *298*, 1912–1934.

(37) Iwatani, M.; Iwata, H.; Okabe, A.; Skene, R. J.; Tomita, N.; Hayashi, Y.; Aramaki, Y.; Hosfield, D. J.; Hori, A.; Baba, A.; Miki, H. Discovery and characterization of novel allosteric FAK inhibitors. *Eur. J. Med. Chem.* **2012**, in press http://dx.doi.org/10.1016/j.ejmech.2012.06.035.

(38) Fragment definition, compound attributes: MW <200; solubility >1µg/ml, number of hydrogen bond donors and acceptors ≤ 3.

(39) Erlanson, D. A.; McDowell, R. S.; O'Brien, T. Fragment-Based Drug Discovery. *J. Med. Chem.* **2004**, *47*, 3463-3482.

(40) The complete FAK-fragment screening will be described elsewhere, manuscript in preparation.

(41) Unpublished results. 43 screening hits could be crystallized successfully and characterized by x-ray analysis.

(42) Initial fragment decorations gave N-Methyl-N-{3-[(7H-pyrrolo[2,3-d]pyrimidin-4-ylamino)-methyl]-pyridin-2-yl}-methanesulfonamide with an affinity of K_D: 3.1 µM and a surprising biochemical IC_{50} of 8.9 µM. The addition of methyl in 'position 2' gave N-Methyl-N-{3-[(6-methyl-7H-pyrrolo[2,3-d]pyrimidin-4-ylamino)-methyl]-pyridin-2-yl}-methanesulfonamide with a significant loss of affinity (K_D: 57 µM). So for IP reasons and technical feasibility neither the pyrazolo-pyrimdine nor the pyrrolo-pyrimidine core were considered for further fragment growing initiatives. It was anticipated that the 1H-N and the 7N are the hinge-binding elements and hence the pyrrolo[2,3-b]pyridine (7-azaindole) should be sufficient to work as hinge-binder.

(43) Popowycz, F.; Routier, S.; Joseph, B.; Mérour, J.-Y. Synthesis and reactivity of 7-azaindole (1H-pyrrolo[2,3-b]pyridine). *Tetrahedron* **2007**, *63*, 1031-1064.

(44) Depending on the availability of starting material slightly modified schemes were followed. **32** and **46** were prepared as outlined in Scheme 3; **34** and **38** were prepared as described in the experimental section.

(45) We had observed in other projects that the cellular activity often depends on the off-rate of the ligand. Accordingly it was anticipated that low micromolar affinity and a $k_{off} = 0.4\ s^{-1}$ is sufficient to show cellular activity. In the subsequent work we decided to analyse in detail those derivatives with respect to solubility, plasma-protein-binding and permeability where a slow off-rate was determined but no cellular activity could be measured.[46]

(46) Data not shown

(47) Stock of this compound was depleted and re-synthesis not possible so that biophysical characterisation could not be done.

(48) Copeland, R. A.; Pompliano, D. L.; Meek, T.D. Drug-taget residence time and its implications for lead optimization. *Nat. Rev. Drug Discov* **2006**, *5*, 730-739.

(49) Stadt-Müller, H.; Betzemeier, B.; Sapountzis, I. WO 2010/058030.

(50) Henrich, B., Bergamaschi, A., Broennimann, C., Dinapoli, R., Eikenberry, E. F., Johnson, I., Kobas, M., Kraft, P., Mozzanica, A. & Schmitt, B. PILATUS: A single photon counting pixel detector for X-ray applications. *Nucl. Instrum. Methods Phys. Res., Sect. A* **2009**, *607*, 247–249.

(51) Kabsch, W. XDS. *Acta. Cryst.* **2010**, *D66*, 125-132.

(52) Collaborative Computational Project, Number 4. "The CCP4 Suite: Programs for Protein Crystallography". *Acta Cryst.* **1994**, *D50*, 760–763.

(53) Nowakowski, J., Cronin, C.N., McRee, D.E., Knuth, M.W., Nelson, C.G., Pavletich, N.P., Rodgers, J., Sang, B.-C., Scheibe, D.N., Swanson, R.V. & Thompson, D.A. Structures of the cancer-related Aurora-A, FAK, and EphA2 protein kinases from nanovolume crystallography. *Structure* **2002**, *10*, 1659–1667.

(54) Bricogne, G., Blanc, E., Brandl, M., Flensburg, C., Keller, P., Paciorek, W., Roversi, P., Sharff, A., Smart, O.S., Vonrhein, C. & Womack, T.O. **2011**. BUSTER version 2.11.1. Cambridge, United Kingdom: Global Phasing Ltd.

(55) Emsley, P. & Cowtan, K. *Coot*: model-building tools for molecular graphics. *Acta Cryst.* **2004**, *D60***,** 2126–2132.

(56) Koolman, H.; Musil, D.; Heinrich, T.; Krier, M.; Reggelin, M. Co-crystal Structures of FAK with a Novel Pyrrolo[2,3-*d*]thiazole. *Acta Cryst. D* **2012** submitted.

(57) de Kloe, G. E.; Bailey, D.; Leurs, R.; de Esch, I. J. P. Transforming fragments into candidates: small becomes big in medicinal chemistry. *Drug Discov. Today* **2009**, *14*, 630-646.

(58) Antonysamy, S. S.; Aubol, B.; Blaney,J.; Browner, M. F.; Giannetti, A. M.; Harris, S. F.; Hébert, N.; Hendle, J.; Hopkins, S.; Jefferson, E.; Kissinger, C.; Leveque, V.; Marciano, D.; McGee, E.; Nájera, I.; Nolan, B.; Tomimoto, M.; Torres, E.; Wright, T. Fragment-based discovery of hepatitis C virus NS5b RNA polymerase inhibitors. *Bioorg. Med. Chem. Lett.* **2008**, *18*, 2990-2995.

(59) Berman, H.M. ; Westbrook, J.; Feng, Z.; Gilliland, G.; Bhat, T.N.; Weissig, H.; Shindyalov, I.N.; Bourne, P.E. The Protein Data Bank. *Nucleic Acids Research*, **2000**, *28*, 235-242.

Table of Contents Graphic

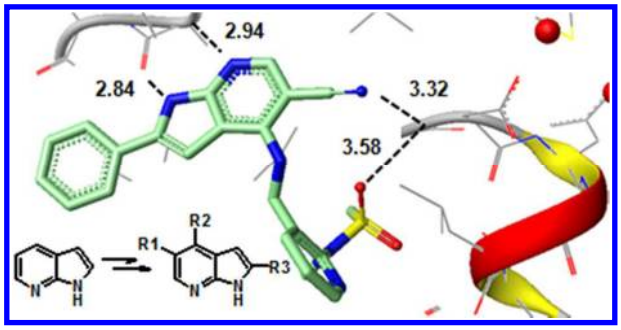

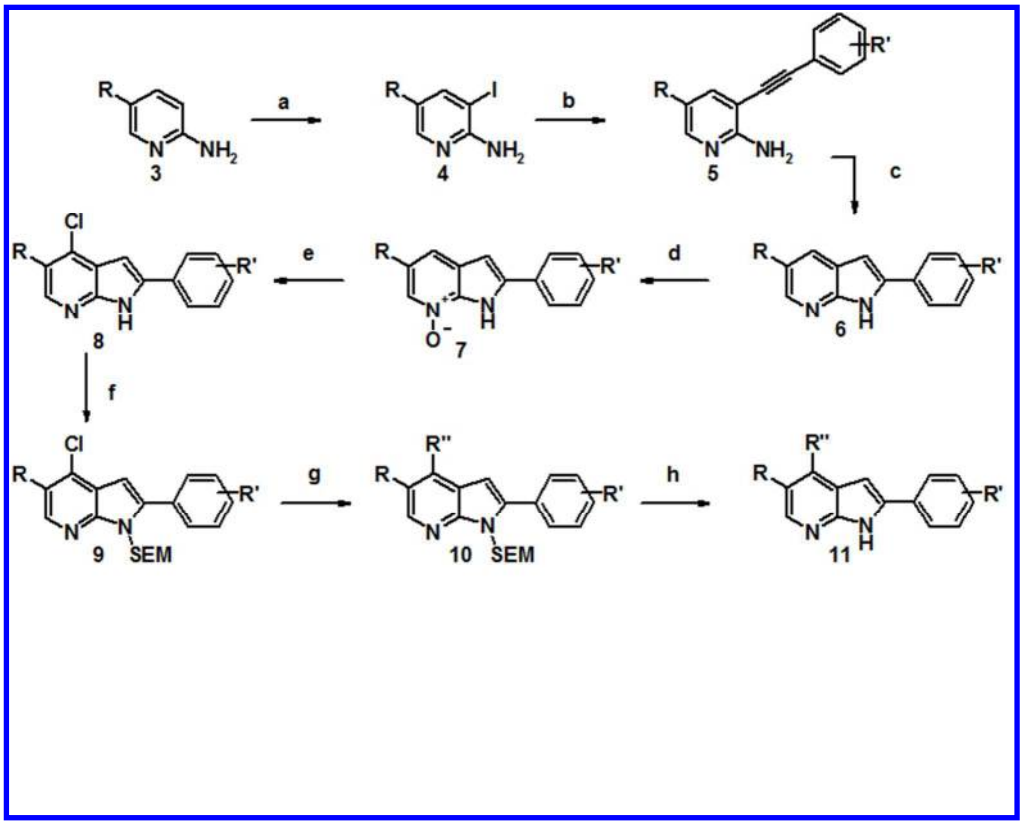

a Reaction conditions: R = CF3, CN; (a) Ag2SO4, I2; (b) R'-phenyl-ethin, PdCl2(PPh3)2, CuI, DMF; (c) NaH, NMP, 60 °C; (d) m-CPBA; (e) POCl3, MsCl, DMF; (f) SEM-Cl, DCM; (g) Cs2CO3, S-Phos, Pd(OAc)2, R''-NH2, dioxane, 150 °C; (h) 4N HCl, THF, reflux, 18 h.
203x162mm (96 x 96 DPI)

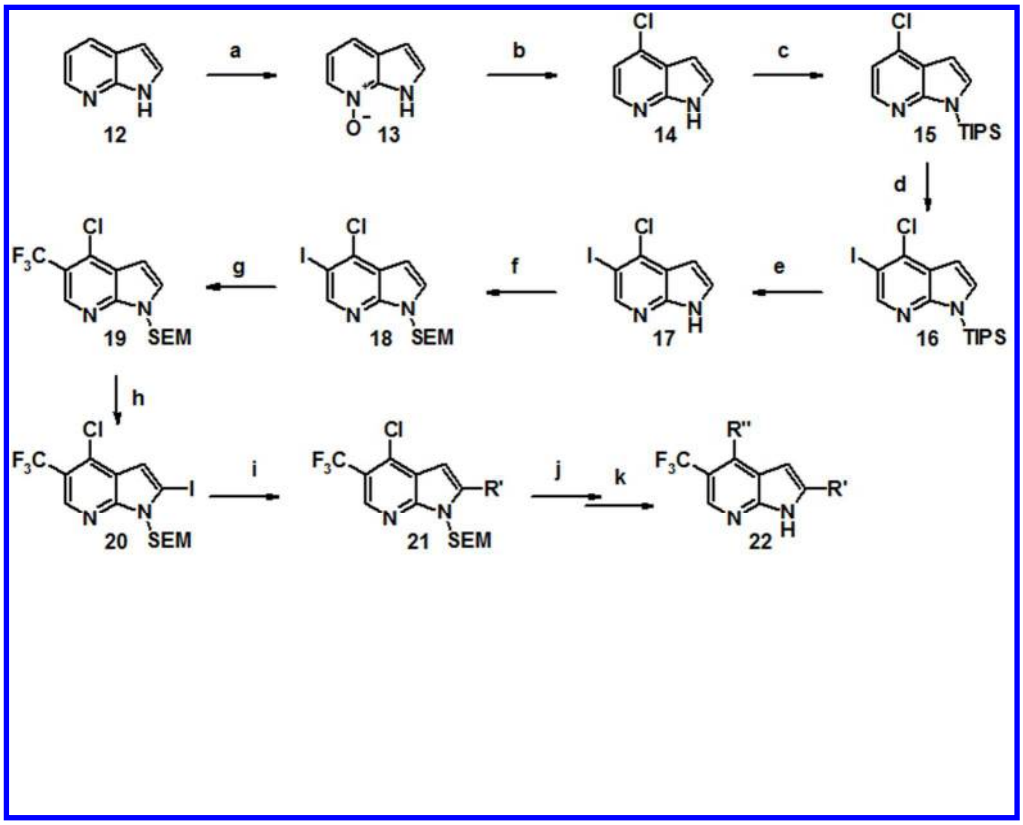

a Reaction conditions: (a) m-CPBA, 0 °C ∀ RT, 77 %; (b) MsCl, DMF, 2 h, 50 °C, 72 %; (c) TIPS-Cl, NaH, THF, 1h, 0 °C, 65 %; (d) sec-BuLi, -78 °C, I2, DMF, 60 %; (e) TBAF, THF, 1 h, 0 °C ∀ RT, 80 %; (f) SEM-Cl, NaH, THF, 0 °C, 2h, 88 %; (g) 2,2-Difluoro-2-(fluorosulfonyl)acetic acid, CuI, DMF, 100 °C, 3 h, 72 %; (h) BuLi, -45 °C, I2, THF, 64 %; (i) Pd(OAc)2, S-Phos, Cs2CO3, R'-B(OH)2, dioxane, H2O, 60°C, 58 %; (j) Pd(OAc)2, Xanthphos, Cs2CO3, R"-NH2, dioxane, H2O, 60 °C, 46 %; k. 4N HCl, THF, reflux, 65 %.
203x162mm (96 x 96 DPI)

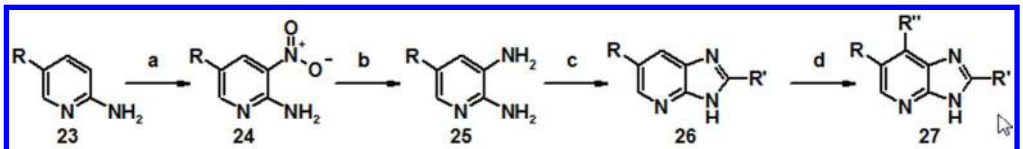

a Reaction conditions: (a) conc. H2SO4/HNO3; (b) Fe, NH4Cl; (c) R`-CHO, PTSA; (d)i: m-CPBA, POCl3; ii: DIPEA, NMP, R``-NH2.
218x162mm (96 x 96 DPI)

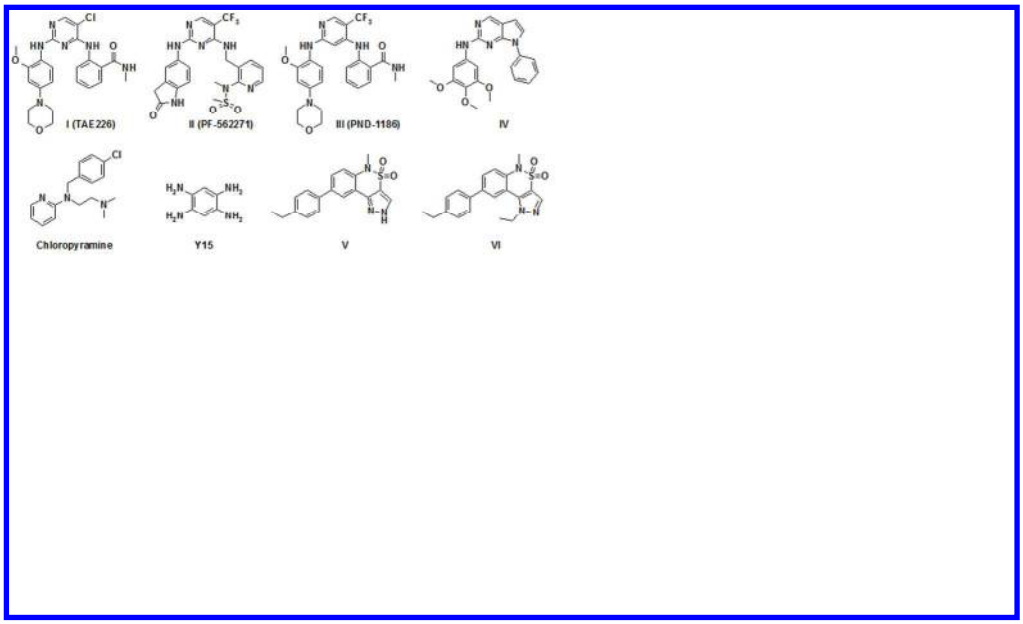

Figure 1. FAK inhibitors
319x191mm (96 x 96 DPI)

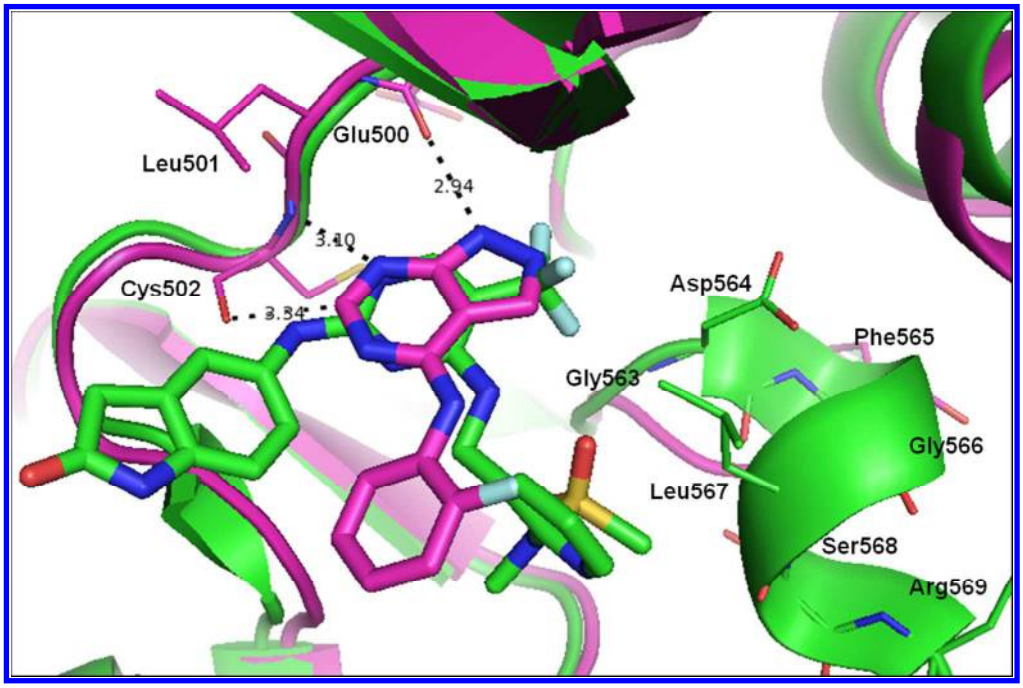

183x122mm (150 x 150 DPI)

Figure 3. Hinge-binding scaffold 1H-pyrazolo[3,4-d]pyrimidine of fragment 1 and 1H-pyrrolo[2,3-b]pyridine template selected for optimization as the lower nitrogen content of the later allows the introduction of more substituents.
319x191mm (96 x 96 DPI)

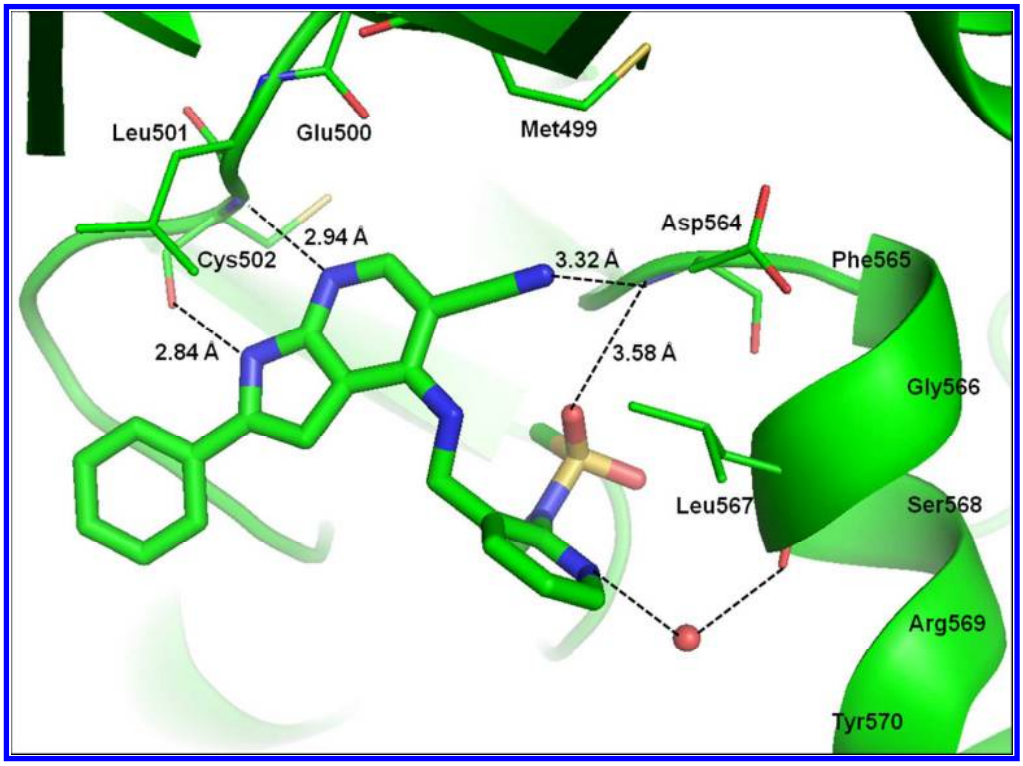

186x138mm (150 x 150 DPI)

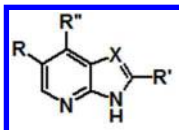

218x162mm (96 x 96 DPI)

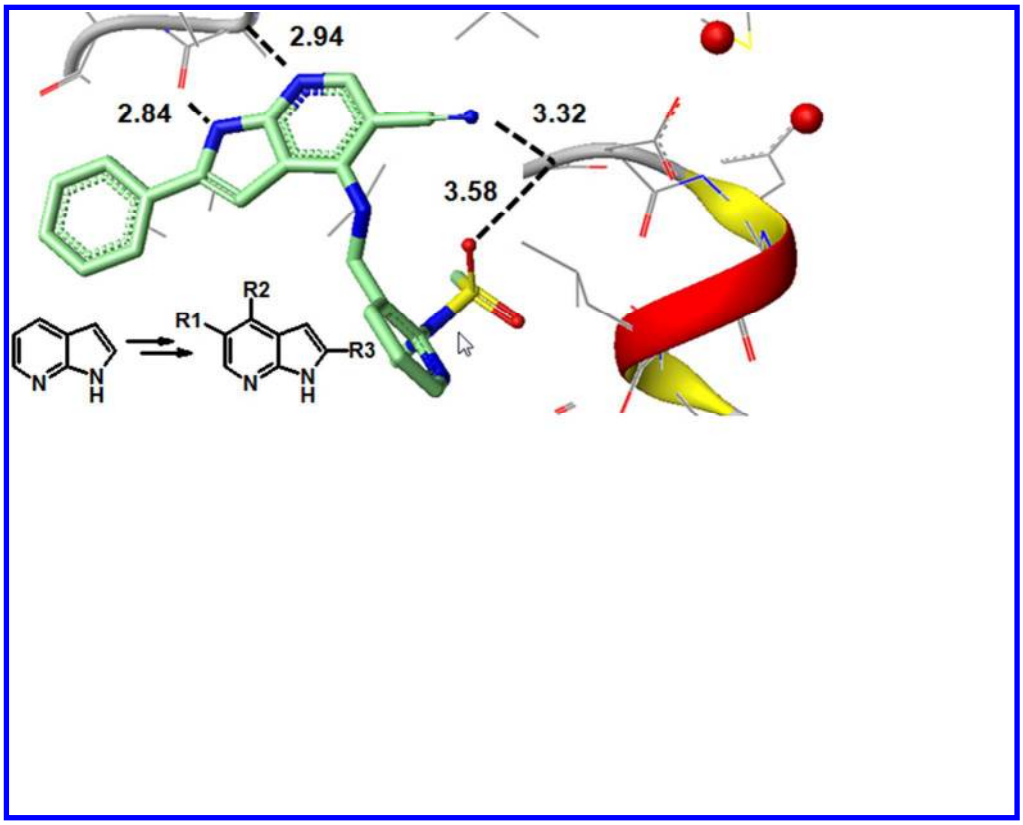

203x162mm (96 x 96 DPI)